Published in final edited form as:
Dev Biol. 2009 March 1; 327(1): 216–227. doi:10.1016/j.ydbio.2008.12.019.

Increased thymus- and decreased parathyroid-fated organ domains in *Splotch* mutant embryos

Ann V. Griffith[1,4,5], **Kim Cardenas**[1,5], **Carla Carter**[1], **Julie Gordon**[2], **Aimee Iberg**[1], **Kurt Engleka**[3], **Jonathan A. Epstein**[3], **Nancy R. Manley**[2], and **Ellen R. Richie**[1,6]

1 *Department of Carcinogenesis, University of Texas MD Anderson Cancer Center, Science Park Research Division, Smithville, TX 78957*

2 *Department of Genetics, B420A Life Sciences Bldg, University of Georgia, Athens, GA 30602*

3 *Department of Cell and Developmental Biology and Penn Cardiovascular Institute, University of Pennsylvania, Philadelphia PA 19104*

Abstract

Embryos that are homozygous for *Splotch*, a null allele of *Pax3*, have a severe neural crest cell (NCC) deficiency that generates a complex phenotype including spina bifida, exencephaly and cardiac outflow tract abnormalities. Contrary to the widely held perception that thymus aplasia or hypoplasia is a characteristic feature of $Pax3^{Sp/Sp}$ embryos, we find that thymic rudiments are larger and parathyroid rudiments are smaller in E11.5–12.5 $Pax3^{Sp/Sp}$ compared to $Pax3^{+/+}$ embryos. The thymus originates from bilateral third pharyngeal pouch primordia containing endodermal progenitors of both thymus and parathyroid glands. Analyses of *Foxn1* and *Gcm2* expression revealed a dorsal shift in the border between parathyroid- and thymus-fated domains at E11.5, with no change in the overall cellularity or volume of each shared primordium. The border shift increases the allocation of third pouch progenitors to the thymus domain and correspondingly decreases allocation to the parathyroid domain. Initial patterning in the E10.5 pouch was normal suggesting that the observed change in the location of the organ domain interface arises during border refinement between E10.5 and E11.5. Given the well-characterized NCC defects in *Splotch* mutants, these findings implicate NCCs in regulating patterning of third pouch endoderm into thymus- versus parathyroid-specified domains, and suggest that organ size is determined in part by the number of progenitor cells specified to a given fate.

Keywords

thymus; parathyroid; neural crest cells; Pax3; pharyngeal pouch endoderm

INTRODUCTION

The thymus provides a unique and indispensable microenvironment for the generation of self-tolerant T cells that comprise an essential component of the adaptive immune response. The

6Corresponding author Phone: 512-237-9435, FAX: 512-237-9444, email: erichie@mdanderson.org.
4Present address: Department of Cancer Biology, Scripps Florida Research Institute, Jupiter, FL 33458
5These authors contributed equally to this work.

thymus and parathyroid glands originate in a bilateral fashion from endoderm of the third pharyngeal pouch (reviewed in (Anderson et al., 2006; Blackburn and Manley, 2004; Manley, 2000). Each third pouch initially forms a common primordium containing thymus- and parathyroid-specific domains. Although epithelial cells of the common primordia are morphologically indistinguishable, patterning of third pouch endoderm into organ-specific domains is apparent from the expression pattern of *Foxn1* and *Gcm2* transcription factors that are restricted to the thymus- and parathyroid-fated domains respectively (Gordon et al., 2001). *In situ* hybridization (ISH) analysis shows that *Gcm2* expression is localized to the anterior and dorsal region of third pouch endoderm, whereas *Foxn1* is expressed in ventral and posterior regions of the third pouch. After the initial patterning is established, the shared primordia detach from the pharyngeal endoderm at approximately embryonic day 12 (E12), shortly after which the thymus and parathyroid rudiments separate from each other. The bilateral thymic lobes undergo medial, ventral and caudal migration to reach their final position above the heart.

Epithelial-mesenchymal interactions are a common theme in the development of various organs including the thymus. NCCs migrate into the vicinity of the third pharyngeal pouches during formation of the common thymus/parathyroid primordia and are a major component of the condensing mesenchymal capsule that surrounds the thymus rudiment after it separates from the parathyroid (Jiang et al., 2000; LeLievre and Le Douarin, 1975). In vitro and in vivo studies have demonstrated that mesenchyme provides essential signals for thymus organogenesis. Removal of mesenchymal cells from intact or reaggregated fetal thymus organ cultures at stages after E12.5 arrests thymus development in vitro (Auerbach, 1960; Jenkinson et al., 2003). *In vivo* ablation of premigratory NCCs in chicks was reported to result in ectopic, hypoplastic or absent thymic lobes (Bockman, 1984).

Perithymic mesenchyme promotes proliferation of the fetal thymus epithelial rudiment resulting in expansion of intrathymic niches that support thymocyte development (Jenkinson et al., 2007). The NCC-derived mesenchymal capsule produces growth factors, Fgf7 and Fgf10 that activate the fibroblast growth factor receptor, FgfR2IIIb expressed on thymic epithelial cells (TECs) (Erickson et al., 2002; Jenkinson et al., 2003; Revest et al., 2001). Outgrowth of the thymic rudiment is arrested by E12.5 and severe thymus hypoplasia is apparent by E18.5 in embryos that express a truncated, inactive isoform of FgfR2IIIb (Revest et al., 2001). The reduced TEC proliferation observed in Fgf10 null embryos further substantiates the link between thymus outgrowth and Fgf signaling (Ohuchi et al., 2000; Revest et al., 2001). Additional factors that are implicated in thymus growth and development include IGF1 and IGF2 produced by PDGFRα positive fetal mesenchyme (Jenkinson et al., 2007), and BMP4 expressed in thymus domain endoderm and adjacent NC-derived mesenchyme (Bleul and Boehm, 2005; Patel et al., 2006; Tsai et al., 2003). These investigations largely address the role of NCCs in supporting growth of the thymic rudiment after E12.5; earlier roles are not yet well defined.

Pax3 is a transcription factor expressed by premigratory neural crest precursors and is required for the survival, proliferation and differentiation of NCCs (Conway et al., 2000; Epstein et al., 2000; Pani et al., 2002). The point mutation *Splotch* (*Sp*) is a null allele of *Pax3* that abolishes protein function (Auerbach, 1954; Goulding et al., 1991). Homozygous *Splotch* embryos are a well-established genetic model of severe neural tube defects and NCC deficiency. $Pax3^{Sp/Sp}$ mutants have a complex phenotype characterized by numerous developmental defects including spina bifida, exencephaly, and cardiac outflow tract abnormalities resulting in embryonic lethality by about E13 (Conway et al., 2000; Epstein et al., 2000). In addition, ectopia and hypoplasia or aplasia of the thymus are considered to be characteristic features of $Pax3^{Sp/Sp}$ embryos (Auerbach, 1954; Conway et al., 1997; Franz, 1989; Machado et al., 2001). Recent reviews reflect a general perception that the thymus is frequently absent or small

in *Pax3*$^{Sp/Sp}$ mutants (Anderson et al., 2006; Hollander et al., 2006). This assessment is consistent with, and indeed part of, the evidence supporting a requirement for NCCs in thymus organogenesis. However, our data demonstrate that thymic lobes in E12.0–E12.5 *Pax3*$^{Sp/Sp}$ embryos, although ectopic, are actually larger than those in *Pax3*$^{+/+}$ littermates. This unexpected phenotype is not a consequence of enhanced proliferation or diminished apoptosis of epithelial cells in the thymus rudiment. Instead, ISH analysis of organ-specific markers demonstrates that the NCC defect in *Pax3*$^{Sp/Sp}$ embryos results in aberrant patterning of the thymus- and parathyroid-fated domains as well as disrupted boundary formation in the shared third pouch primordium. These findings suggest that NCCs are involved in patterning third pouch endoderm by regulating the spatial and temporal expression of transcription factors that influence thymus versus parathyroid fate specification of pouch endoderm.

MATERIALS AND METHODS

Mice

Pax3$^{Sp/+}$ mice on a C57Bl6/J background were purchased from The Jackson Laboratory (Bar Harbor, ME) and crossed to generate *Pax3*$^{Sp/Sp}$ embryos and littermate controls. Noon of the day the vaginal plug was found was designated as embryonic day 0.5. Embryos were also staged by morphological criteria including somite number and eye and limb morphology.

In Situ Hybridization

Embryos were collected in PBS containing 0.1% Tween20 and fixed in 4% paraformaldehyde overnight. They were dehydrated in a series of 30%, 50%, 70%, 90%, and 100% ethanol and paraffin embedded. ISH was performed on slides using digoxygenin-labeled antisense riboprobes constructed from linearized plasmids containing cDNA templates for mRNA probe production, as previously described (Zamisch et al., 2005), except that the proteinase K digestion was omitted. The *CrabP1* (cellular retinoic acid binding protein I), *IL-7*, *Foxn1*, *Gcm2* and *Bmp4* probes have been described (Alpdogan et al., 2006; Gordon et al., 2001; Leonard et al., 1995; Zamisch et al., 2005). Each ISH analysis was performed on at least three *Pax3*$^{Sp/Sp}$ mutants and two wildtype littermates. Sections were counterstained with nuclear fast red.

Three-dimensional reconstructions

Three-dimensional reconstructions were created by tracing digital images captured from serial sections of paraffin embedded tissue stained by H&E or ISH using Surf Driver (version 3.5.2) software (www.surfdriver.com). For E12.5 embryos, tracings of the trachea, esophagus and thyroid along with thymus lobes and parathyroids were used for consistent alignment. For E11.5 samples, pouch lumens were aligned. At least three embryos were analyzed at each developmental stage and one three-dimensional reconstruction was chosen for presentation.

Histochemistry and Immunohistochemistry

Sections were stained with hematoxylin and eosin (H&E) by standard techniques. For immunohistochemical staining, embryos were placed in OCT compound and 5μm sections were cut. Sections were fixed with acetone. Sections were stained with primary antibodies from the following sources: rabbit anti-mouse K5 (Covance Research; Richmond, CA); rat anti-K8 (Troma-1; Developmental Studies Hybridoma Bank; Iowa City, IA); rat anti-mouse major histocompatibility complex (MHC) class II (clone M5/114.15.2), rat anti-c-kit (clone ACK45), and rat anti-CD45 (30-F11) were purchased (clone MEC13.3) (BD Biosciences; San Diego, CA); mouse anti-pancytokeratin (clone C-11) (Sigma; Saint Louis, MO). MHC class II, PDGFRα and CD45 immunoreactivity was enhanced by biotinyl tyramide amplification (TSA kit; PerkinElmer Life Sciences; Boston, MA) and detected with streptavidin-fluorescein

isothiocynate (FITC). Second step anti-immunoglobulin (anti-Ig) reagents included Texas Red (TxR) conjugated donkey anti-rabbit and donkey anti-rat Ig, as well as FITC conjugated donkey anti-mouse and donkey anti-rabbit Ig (Jackson ImmunoResearch Laboratories, West Grove, PA). Controls included slides incubated with species or isotype-matched mouse Ig. For costaining, sections were incubated simultaneously with primary Abs from different species. Microscopic analysis was performed with an Olympus ProVis AX70 microscope (Olympus, Melville, NY).

Apoptosis and Proliferation Assays

TUNEL staining was performed using the In Situ Cell Death Detection Kit (Roche, Mannheim, Germany). Frozen sections were fixed in 4% paraformaldehyde for 30 min at room temperature. The slides were rinsed in PBS and permeabilized with 0.1% Triton X 100/0.1% sodium citrate on ice for 2min. After an additional rinse with PBS, the slides were treated with solution A and B and incubated in the dark at 37°C according to manufacturers instructions. Proliferation was assessed by indirect immunofluorescence. Frozen sections from E11.5 *Splotch* and wildtype littermates were incubated with DAPI to detect nuclei and with rabbit anti-phosphohistone H3 (Upstate; Lake Placid, NY) followed by FITC-conjugated donkey anti-rabbit Ig (Jackson ImmunoResearch Laboratories, West Grove, PA) to detect mitotic cells (Hendzel et al., 1997).

RESULTS

Thymus lobes in Pax3$^{Sp/Sp}$ embryos are ectopic but not hypoplastic

After the common thymus-parathyroid primordia detach from the pharyngeal endoderm the developing thymus and parathyroid glands separate from each other while the thymic rudiments undergo ventral, medial and caudal migration toward the ventral pharynx. By E12.5, wildtype thymic lobes are located cranial to the heart and caudal to the laryngeo-tracheal groove (Fig. 1A). Consistent with earlier reports that NCC defects in *Pax3*$^{Sp/Sp}$ mice produce thymus aplasia or hypoplasia, we found no thymic tissue at a comparable position in *Pax3*$^{Sp/Sp}$ littermates (Fig. 1B). However, inspection of more anterior sections revealed surprisingly large *Pax3*$^{Sp/Sp}$ thymic lobes above the laryngeo-tracheal groove (anterior to the separation of the trachea and esophagus) (Fig. 1D). In contrast, only the anterior tip of the wildtype thymus was evident at a similar position (Fig. 1C).

To better visualize the relative dimensions and position of thymus lobes in E12.5 *Pax3*$^{Sp/Sp}$ and *Pax3*$^{+/+}$ littermates, we generated 3-D reconstructions of the pharyngeal region using serial transverse sections (Fig. 1E, F). The results confirm that caudal migration of *Pax3*$^{Sp/Sp}$ thymus primordia is defective compared to their wildtype counterparts. We also found that, consistent with the larger size of mutant thymus lobes observed in histological sections, there is a significant increase in the volume of *Pax3*$^{Sp/Sp}$ thymus lobes compared to *Pax3*$^{+/+}$ controls (Fig. 1G). Conversely, the *Pax3*$^{Sp/Sp}$ parathyroid primordia were smaller in volume than those of wildtype littermates (Fig. 1H). These results demonstrate that contrary to expectations, thymus aplasia or hypoplasia is not a typical consequence of the NCC defect in *Splotch* mutants.

During normal ontogeny, the third pouch-derived thymus-parathyroid shared primordia detach from the pharynx at around E12. Inspection of H&E stained transverse sections showed that separation of these shared primordia from pharyngeal endoderm was delayed in four of six *Pax3*$^{Sp/Sp}$ embryos but none of six *Pax3*$^{+/+}$ littermates (compare Fig. 2 B, D with Fig. 2A, C). To determine whether delayed detachment from the pharynx was specific to the third pouch-derived shared primordia or reflected a general pharyngeal pouch defect, we examined the ultimobranchial bodies, which are derived from the fourth pharyngeal pouch and normally detach from the pharynx prior to detachment of the thymus lobes. The normal detachment of

ultimobranchial bodies observed in *Splotch* mutant embryos (Fig. 2E, F) demonstrates that the separation defect is restricted to the third pouch-derived thymus-parathyroid primordia. These results suggest that delayed separation from pharyngeal endoderm likely contributes to the ectopic position of *Pax3*$^{Sp/Sp}$ thymus lobes.

Perithymic NCC localization and capsule formation are deficient in Pax3$^{Sp/Sp}$ embryos

The fetal thymus rudiment is encompassed by a NC-derived mesenchymal capsule that provides essential signals to the developing thymic epithelial compartment (Auerbach, 1960; Foster et al., 2008; Jenkinson et al., 2007). Thymic sections were stained with anti-PDGFRα to detect the NC-derived mesenchymal capsule surrounding the cytokeratin positive thymus epithelial rudiment in E12.5 *Pax3*$^{Sp/Sp}$ and *Pax3*$^{+/+}$ littermates. Figure 2G shows abundant PDGFRα positive mesenchymal cells encompassing the wildtype thymic epithelial rudiment. In contrast, there is a striking deficiency in NC-derived perithymic cells as shown by the paucity of PDGRFα expressing cells adjacent to the *Pax3*$^{Sp/Sp}$ thymic rudiment (Fig. 2H). However, the presence of DAPI stained nuclei indicates the presence of other cell types proximal to the *Pax3*$^{Sp/Sp}$ thymic epithelial rudiment. These results confirm that the NCC defect in these mutants directly affects the contribution of mesenchyme to the early thymic rudiment.

To compare the pattern of NCC migration in the vicinity of the third pouch in E10.5 *Pax3*$^{Sp/Sp}$ and *Pax3*$^{+/+}$ embryos, we assessed expression of *CrabP1*, a marker for migrating NCCs ISH analysis showed that NCCs were abundant in the dorsal region of the third pouch in E10.5 *Pax3*$^{+/+}$ embryos (Fig. 3A, C). In contrast, there was a notable reduction of NCCs in the vicinity of the third pharyngeal pouch in E10.5 *Pax3*$^{Sp/Sp}$ mutants (Fig. 3B,D). These data are consistent with a previous report showing a reduction in NCCs populating the pharyngeal arches and cardiac outflow tract of *Pax3*$^{Sp/Sp}$ embryos (Epstein et al., 2000). By E11.5, NCCs were predominantly localized in the ventral region of the third pouch in wildtype embryos indicating a dorsal to ventral axis of migration, but were still dramatically reduced in the mutants (data not shown).

Differentiation of thymic epithelium is not impaired in Pax3$^{Sp/Sp}$ embryos

Since NC-derived mesenchyme has been implicated in TEC differentiation and function, we performed an immunohistochemical analysis to evaluate TEC differentiation in the ectopic thymic rudiment of *Pax3*$^{Sp/Sp}$ embryos. At E12.5 the thymic anlage consists predominantly of TECs that express cytokeratin 8 (K8), but not K5 as well as a central region of K8^{+}K5^{+} TECs that contain progenitors of mature cortical and medullary TECs (Bennett et al., 2002; Gill et al., 2002) (Fig. 4A). Both K8^{+}K5^{-} and K8^{+}K5^{+} TEC subsets were present in E12.5 *Pax3*$^{Sp/Sp}$ thymus lobes (Fig. 4B). The keratin expression pattern was correctly established even when the mutant thymic lobes failed to separate from the pharynx, indicating that separation from the pharyngeal endoderm is not required for TEC differentiation (Fig. 4C).

To obtain functional evidence of TEC differentiation, we examined MHC class II and interleukin-7 (IL-7) expression, as well as the timing of hematopoietic precursor cell (HPC) immigration. MHC class II expression is required for thymocyte selection and is normally initiated at approximately E12.5 (Shinohara and Honjo, 1997). MHC Class II expression was comparable in the *Pax3*$^{Sp/Sp}$ and *Pax3*$^{+/+}$ fetal thymus lobes (Fig. 4D, E). IL-7 is a cytokine produced by TECs and required for thymocyte survival, proliferation and differentiation (Fry and Mackall, 2002). We previously found that IL-7 mRNA is highly expressed throughout wildtype thymic lobes at E12.5 (Zamisch et al., 2005). There was a comparable distribution of *IL-7* expressing TECs in *Pax3*$^{Sp/Sp}$ and *Pax3*$^{+/+}$ thymic rudiments (Fig. 4F, G). HPCs are recruited into the thymus beginning at approximately E11.5 in a process that depends on the production of chemokines such as CCL25 and CCL19 by TECs (Liu et al., 2006). A comparable influx of CD45 positive HPCs was observed in the thymic lobes of E12.0 *Pax3*$^{Sp/Sp}$ and

Pax3$^{+/+}$ embryos (Fig. 4H, I). Therefore, *Pax3*$^{Sp/Sp}$ TECs are capable of attracting HPC to migrate across the perithymic mesenchyme into the thymus rudiment. Similar results were obtained when thymocyte progenitors were detected by expression of c-kit confirming that *Pax3*$^{Sp/Sp}$ thymus lobes recruit HPCs (data not shown). Taken together, these results indicate that early TEC differentiation and function are intact in the early ectopic *Pax3*$^{Sp/Sp}$ thymus rudiment.

Proliferation and cellularity are comparable in third pharyngeal pouch endoderm of Pax3$^{Sp/Sp}$ and Pax3$^{+/+}$ littermates

To investigate whether increased epithelial cell proliferation contributed to the unexpectedly large thymus lobes in Pax3$^{Sp/Sp}$ embryos, we determined the frequency of dividing cells in the shared thymus/parathyroid primordia of *Pax3*$^{Sp/Sp}$ and *Pax3*$^{+/+}$ embryos using phosphorylated histone H3 as a marker of mitotic cells (Hendzel et al., 1997). Frozen sections from three *Pax3*$^{Sp/Sp}$ and three *Pax3*$^{+/+}$ E11.5 embryos were co-stained with anti-K8 and DAPI to identify the third pouch and with anti-phosphorylated histone H3 (Fig. 5A–D). Approximately 1.5% of third pharyngeal pouch cells were in mitosis in both *Pax3*$^{Sp/Sp}$ and wildtype littermates (Fig. 5F). To determine if the increased size of *Pax3*$^{Sp/Sp}$ thymus lobes was associated with a decrease in apoptosis, the TUNEL assay was performed on E12.0 frozen thymus sections. At this stage there is little apoptosis in the thymus, and there was no difference in the frequency of apoptotic cells in Pax3$^{Sp/Sp}$ compared *Pax3*$^{+/+}$ thymic rudiments (data not shown). Importantly, the average total number of cells in the combined thymus and parathyroid domains of the E11.5 littermates was not significantly different in Pax3$^{Sp/Sp}$ mutants compared to *Pax3*$^{+/+}$ littermates (Fig. 5E). These data indicate that the Pax3$^{Sp/Sp}$ third pharyngeal pouch does not differ from wildtype in the frequency of proliferating or apoptotic cells or in the total size of the shared primordium.

Defects in the location and shape of the interface between thymus and parathyroid-fated domains in the common primordium of Pax3$^{Sp/Sp}$ embryos

Although there is convincing evidence that NCCs produce growth factors required for outgrowth of the thymus rudiment after E12.5, it is not known if NCCs play an earlier role by influencing patterning of third pharyngeal pouch endoderm into thymus and parathyroid domains. To examine this issue, we analyzed *Gcm2* and *Foxn1* expression domains in the common thymus/parathyroid primordia of *Pax3*$^{Sp/Sp}$ embryos. ISH analysis was performed on serial sagittal sections from *Pax3*$^{+/+}$ and *Pax3*$^{Sp/Sp}$ littermates at E11.5, the earliest stage at which the *Foxn1* thymus-specific marker is expressed. At this developmental stage, the majority of cells in the common primordia express either *Foxn1* or *Gcm2* (compare A with Fig. 6C and Fig. 6B with Fig. 6D). Interestingly, we found an increase in the *Foxn1*-expressing thymus domain of the third pouch-derived primordium in *Pax3*$^{Sp/Sp}$ compared to *Pax3*$^{+/+}$ littermates (Fig. 6A, B), with a corresponding decrease in the *Gcm2* expressing parathyroid domain (Fig. 6C, D). Similar results were obtained in four *Pax3*$^{Sp/Sp}$ mutants and *Pax3*$^{+/+}$ controls at this stage.

To better visualize the relative proportions of the *Foxn1* and *Gcm2* expression domains in the common thymus/parathyroid primordia, three-dimensional images were reconstructed from the ISH data obtained on alternating serial sagittal sections from E11.5 *Pax3*$^{Sp/Sp}$ and *Pax3*$^{+/+}$ littermates. These reconstructions show a marked dorsal shift in the location of the border between thymus and parathyroid fated domains in *Pax3*$^{Sp/Sp}$ common primordia resulting in a relative expansion of the *Foxn1* expressing domain at the expense of the parathyroid domain (Fig. 6E, F). *Foxn1* expressing cells occupied 71±5.0% (n=5) of the wildtype third pharyngeal pouch, but 78±2.8% (n=5) of Pax3 deficient pouch ($p<0.003$). Conversely, *Gcm2* expressing cells occupied 28.8±5.2% of the wildtype pouch, but 21.2±2.8% of Pax3 deficient pouch ($p<0.01$). Importantly, we found that the common third pharyngeal

pouches in wildtype and *Pax3*$^{Sp/Sp}$ mutants are comparable in volume (Fig. 6G). Thus, the altered border position reflects a relative increase in allocation of third pouch endodermal cells to a thymus fate resulting in a corresponding decrease in third pouch endodermal cells fated to become parathyroid.

We also analyzed third pharyngeal pouch patterning in *Pax3*$^{Sp/Sp}$ embryos prior to the initial appearance of *Foxn1* transcripts at E11.25. *Gcm2* is expressed in a discrete domain of the third pouch endoderm of wildtype embryos at E10.5 (Gordon et al., 2001) (Fig. 7C). Although *Foxn1* is not expressed at E10.5, the thymus domain is marked by the expression of *Bmp4* at this stage (Alpdogan et al., 2006; Moore-Scott and Manley, 2005). In wildtype embryos at E10.5, *Bmp4* expression is confined to the ventral posterior thymus domain (Fig. 7A). In contrast to the restricted *Gcm2* and expanded *Foxn1* domains at E11.5, both *Gcm2* and *Bmp4* expression in the third pharyngeal pouch of *Pax3*$^{Sp/Sp}$ mutants were similar to *Pax3*$^{+/+}$ littermates at E10.5 (Fig. 7B, D). These results suggest that initial third pouch patterning is independent of NCC-derived signals.

In addition to the altered location of the thymus/parathyroid interface at E11.5, abnormal arrangement of thymus- and parathyroid-specified domains at the boundary was frequently observed within Pax3$^{Sp/Sp}$ third pouch primordia. Whereas there is a well delineated, straight boundary between the thymus- and parathyroid-fated domains in the third pharyngeal pouch of *Pax3*$^{+/+}$ embryos, the interface in *Pax3*$^{Sp/Sp}$ mutants is uneven. Figure 8 shows an example in which a portion of the *Foxn1* expressing domain is interspersed with the *Gcm2* expressing domain in the dorsal aspect of the pouch, rather than restricted to the ventral aspect of the primordium (Fig. 8B, D). Moreover, the *Foxn1* expression domain was expanded well into the pharyngeal endoderm in some *Pax3*$^{Sp/Sp}$ mutants (Figure 8E). *Foxn1* expression is never detected in non-pouch pharyngeal endoderm of wildtype embryos. Taken together, these data implicate NCC-derived signals in regulating the formation and/or maintenance of a discrete boundary between thymus- and parathyroid-fated domains in the shared third pouch primordia.

Thymus lobes in Pax3$^{Cre/Cre}$ embryos are ectopic but not hypoplastic

Since Pax3$^{Sp/Sp}$ embryos do not survive beyond E12.0–E12.5, it was not possible to directly determine the size and position of thymic lobes at later developmental stages. Therefore, we analyzed thymus development in Pax3$^{Cre/Cre}$ in which replacement of the first coding exon of *Pax3* with a gene encoding Cre recombinase generates a null allele that fails to produce Pax3 protein (Engleka et al., 2005). Homozygous Pax3$^{Cre/Cre}$ embryos have severe neural tube and other NCC-associated defects, but survive several days longer than Pax3$^{Sp/Sp}$ embryos, perhaps due to the mixed genetic background in which modifier genes reduce the severity of cardiac defects. Similar to the Pax3$^{Sp/Sp}$ mutants, the E12.5 Pax3$^{Cre/Cre}$ thymus lobes are ectopic and larger than their wildtype littermates (data not shown). To determine whether thymus lobes become hypoplastic in older embryos, thymus development was assessed at E14.5. Interestingly, well developed thymus lobes are apparent in Pax3$^{Cre/Cre}$ embryos at this later developmental stage (Fig. 9A, B). Furthermore, analysis of 3D reconstructions revealed no significant difference in the volume of wildtype (435±15 10^{-4}mm^3; n=4) versus Pax3$^{Cre/Cre}$ (337±19 10^{-4}mm^3; n=4) thymus lobes at E14.5. This phenotype is discussed in more detail below.

DISCUSSION

Contrary to the generally held view that thymus aplasia or hypoplasia is a typical developmental anomaly in *Splotch* embryos, this report demonstrates that well-developed thymic lobes are present, but located in an ectopic anterior position. Given that the *Splotch* mouse is a well-characterized model of NC deficiency and that previous studies showed NC-derived mesenchyme is required for outgrowth of the E12.5 thymus rudiment (Erickson et al., 2002;

Jenkinson et al., 2003; Jenkinson et al., 2007; Revest et al., 2001), it is not surprising that thymus development was assumed to be impaired in *Pax3*$^{Sp/Sp}$ embryos. However, prior studies did not examine the earliest stages of organogenesis when thymus- and parathyroid-fated endodermal cells occupy ventral and dorsal regions respectively of the third pharyngeal pouch primordia. The present report implicates NCCs in the previously unappreciated role of regulating the patterning of third pharyngeal pouch endoderm into thymus- and parathyroid-fated domains after pouch formation.

Although normal expression of organ-specific markers in third pouch primordia of E10.5 *Pax3*$^{Sp/Sp}$ mutants indicates that initial establishment of thymus- and parathyroid-fated domains is independent of NCC-derived signals, the final position of the border between thymus and parathyroid specific domains is shifted dorsally by E11.5, resulting in a relatively smaller *Gcm2* expressing domain and a correspondingly larger *Foxn1* expressing domain. This shift is not associated with changes in cell death or proliferation. Moreover, overall volumes of E11.5 third pouch-derived primordia were comparable in wildtype and *Pax3*$^{Sp/Sp}$ embryos. Taken together these findings indicate that more endodermal cells in the shared third pouch of *Splotch* mutants are specified to a thymus fate and fewer cells are specified to a parathyroid fate. This border shift accounts for the unexpectedly large thymus and smaller parathyroid rudiments observed in E12.5 *Pax3*$^{Sp/Sp}$ embryos. Moreover, the normal third pouch patterning observed in *Pax3*$^{Sp/Sp}$ embryos at an earlier developmental stage, E10.5, is consistent with our previous and current data showing that not all cells in the third pouch express Gcm2 or Bmp4 at this stage (Fig. 7 and (Gordon et al., 2001). This phenomenon results in an ‘unspecified’ central region at E10.5 that expresses neither organ-specific marker. Since all cells in the primordium express an organ-specific marker by E11.5, we propose that additional patterning events occur between E10.5–11.5, in which the precise location of the final boundary between the thymus and parathyroid domains is set. The current data strongly suggest that signals from NCCs are required for the final position of this boundary.

The notion that unique NCC-derived signals are not essential for thymus fate specification is supported by investigations showing the development of a functional thymus following transplantation of isolated pharyngeal endoderm obtained prior to NCC migration (Gordon et al., 2004; LeLievre and Le Douarin, 1975). Moreover, the NCC deficiency in *Splotch* mutant mice does not impair *Foxn1* expression. Indeed, our results suggest that thymus fate specification is a NCC-independent process, since the presumptive thymus-specific domain as marked by *Bmp4* expression is unaffected in the *Pax3*$^{Sp/Sp}$ mutants. During normal pouch patterning, *Foxn1* is first expressed in the cells located at the distal end of the third pouch primordia and expands dorsally to the *Gcm2* expression boundary (Gordon et al., 2001). This process appears to be operative in the *Pax3*$^{Sp/Sp}$ common primordia, resulting in a situation in which reduction of the *Gcm2* expression domain in the *Pax3*$^{Sp/Sp}$ common primordia at E11.5 is compensated for by a relative expansion of the *Foxn1* expression domain. This model could also explain the mixing of *Gcm2* and *Foxn1* expression domains that we frequently observe in *Pax3*$^{Sp/Sp}$ common primordia. Since NCC migration and function are not completely abrogated in *Pax3*$^{Sp/Sp}$ mutants, there is a small probability that any given NCC can migrate to a position proximal to the dorsal region of the common primordia and generate signals that affect gene expression patterns in the endoderm. However, since appropriate migration and function of *Pax3*$^{Sp/Sp}$ NCCs would be a stochastic process, nonconsecutive portions of dorsal endoderm would receive sufficient NCC-derived signals to affect patterning during the later boundary refinement phase, resulting in an apparent mixing of fate domains.

At first glance, our findings appear to be at odds with the notion that NCC deficiency results in thymus hypoplasia. A likely explanation for this paradox is that NCCs perform distinct functions during early patterning of the common primordia compared to later outgrowth of the thymic rudiment. Our evidence suggests that whereas NCC-derived signals do not play a direct

role in initially committing third pouch endodermal progenitors to a thymus or parathyroid fate, they play an essential role in refining these domains between E10.5 and E11.5. It has been shown that by E12, perithymic mesenchyme produces growth factors IGF1 and IGF2 that are thought to induce growth of the early thymus rudiment (Jenkinson et al., 2007). Subsequently, at E13.5–E14, TECs upregulate FgfR2-IIIb expression and the mesenchymal capsule produces Fgf7 and Fgf10 to promote TEC proliferation (Jenkinson et al., 2003; Revest et al., 2001). Taken together, these data suggest that the functional role of NC-derived perithymic mesenchyme evolves throughout thymus organogenesis.

Although there is a severe reduction in NCC-derived mesenchyme in these mutants, mesoderm-derived mesenchyme remains. This raises the interesting possibility that some of the phenotypes seen could be due to the new proximity of mesoderm-derived factors to endoderm (a dominant effect), or could be mitigated by similar factors produced by both types of mesenchyme (a redundancy effect). One instance in which this issue may be important is at later stages in the *Pax3*$^{Cre/Cre}$ mice. It is not clear why the Pax3$^{Cre/Cre}$ thymus lobes do not maintain a comparatively larger volume at the later developmental stage. One possibility is that growth factors produced locally by mesodermal mesenchyme have limited ability to compensate for a deficiency in NC-derived growth factors. Alternatively, a physical reduction in the NCC mesenchyme capsule may provide inadequate signals for thymic epithelial cell growth, causing a slightly slower rate of growth for Splotch-derived stromal cells. While this reduction might result in a gradual thymic hypoplasia, the initially larger target size may mitigate the slower growth. In any case, the Pax3$^{Cre/Cre}$ model of NC deficiency confirms the *Splotch* data at E12.5 and shows that NC deficiency does not result in thymus hypoplasia in late gestation embryos.

Our results in *Splotch* mutants strongly suggest that NCC-derived signals are not essential for initial differentiation of TECs. The thymic epithelial rudiment in *Pax3*$^{Sp/Sp}$ embryos expresses several functional differentiation markers and supports the influx of HPCs. Distinct TEC subsets defined by keratin expression pattern develop in *Pax3*$^{Sp/Sp}$ mutants even when the thymic rudiment fails to detach from the pharyngeal endoderm. These observations are consistent with previous reports showing that sustained mesenchymal/TEC interactions are not required to support differentiation of immature TECs into functional cortical and medullary subsets (Jenkinson et al., 2003; Jenkinson et al., 2007). In contrast, a recent study reported impaired expression of MHC class II and other functional molecules in E13 embryos that are homozygous for the *Patched* deletion that disrupts the PDGFRα gene resulting in aberrant migration and increased apoptosis of NCCs (Itoi et al., 2007). The apparent discrepancy between the earlier report and our data may be due to the fact that the *Patched* deletion encompasses other relevant genes including *c-kit* (Nagle et al., 1994).

To our knowledge this is the first evidence implicating NCCs in patterning the third pouch endoderm into organ-specific domains. The results are reminiscent of our previous data showing that formation of the parathyroid-specific domain depends on signals from Shh produced by pharyngeal endoderm (Moore-Scott and Manley, 2005). It is possible that Shh acts in part through NCC mesenchyme to establish the parathyroid domain in the third pouch. Shh signaling to both the NCC and/or directly to the endoderm may be integrated to pattern the parathyroid domain in the third pouch endoderm. Separate NCC-derived signal(s) downstream of Shh would then act to set the parathyroid organ domain boundaries. Since NCCs are primarily located adjacent to the dorsal third pouch by E10.5 in both wildtype and mutant embryos, and Shh expression is restricted to the pharynx and excluded from the pouch itself, parathyroid fate is restricted to the dorsal domain. In *Pax3*$^{Sp/Sp}$ embryos, reduction or absence of NCC-derived signals could result in a shift in the final location of the parathyroid-thymus border within the pouch, resulting in a smaller *Gcm2* expressing parathyroid domain. Thus, the NCC defect in *Pax3*$^{Sp/Sp}$ embryos ultimately results in an altered allocation of organ specific

domains of the third pouch common primordia, with an increase in the thymus domain at the expense of the parathyroid domain.

The ectopic location of the thymic rudiments in *Pax3*$^{Sp/Sp}$ embryos likely accounts for the widely held, but erroneous perception that thymus hypoplasia or aplasia is a general phenotypic feature in *Splotch* mutants. Thymus ectopia can be caused either by delayed separation from the pharynx, or by a direct defect in migration, or both. The NCC deficiency in *Pax3*$^{Sp/Sp}$ embryos disrupts whatever mechanism is required for apoptosis and separation of the primordium from the pharynx at some frequency. Although we did not observe a decreased frequency of apoptotic cells within the thymic rudiment, the coordinated apoptosis required for this separation event occurs outside the primordium in a brief window at E12 (Gordon et al., 2004). Thus, the observed phenotype is likely due to changes in the timing or extent of apoptosis at the junction of the primordium and the pharynx in mutant embryos. Thymus ectopia could also result from a separate defect in migration of the separated thymus rudiment, which has also been associated with NCC defects.

Early investigations suggested that NCCs regulate segmentation and organization of pharyngeal endoderm into arches and pouches (reviewed in (Graham et al., 2004). However, neural crest ablation does not prevent pharyngeal arch development (Veitch et al., 1999). Since segmentation of pharyngeal endoderm is a general characteristic of chordates (Schaeffer, 1987), occurring prior to the evolutionary development of neural crest, perhaps it is not surprising that the pharyngeal endoderm has an intrinsic morphogenetic capacity. However, a role for NCCs in influencing the patterning of pouch endoderm into organ specific domains and in promotion of initial organogenesis remains possible. The data obtained using the NC deficient *Splotch* model implicates NCCs in a previously unrecognized role, that of final patterning third pharyngeal pouch endoderm into thymus- and parathyroid-fated domains. Although recent considerations of pharyngeal arch patterning have emphasized that pouch formation and anterior-posterior identity are established independently of NCCs, these findings refocus attention on the potential role of NCCs in regulating patterning of pharyngeal pouch endoderm.

Acknowledgements

We thank Francesca Vitelli and A. Baldini for advice and helpful discussions (Baylor College of Medicine). We thank Becky Brooks for assistance in manuscript preparation. This work was supported in part by grants as follows: NIEHS (ES07784), NCI (CA16672), NIH (HD056315) and by the Rothman/Stevenson fund to E.R.R. and as well as by NIH (HD035920) to N. R. M.

References

Alpdogan O, Hubbard VM, Smith OM, Patel N, Lu S, Goldberg GL, Gray DH, Feinman J, Kochman AA, Eng JM, Suh D, Muriglan SJ, Boyd RL, van den Brink MR. Keratinocyte growth factor (KGF) is required for postnatal thymic regeneration. Blood 2006;107:2453–60. [PubMed: 16304055]

Anderson G, Jenkinson WE, Jones T, Parnell SM, Kinsella FA, White AJ, Pongrac'z JE, Rossi SW, Jenkinson EJ. Establishment and functioning of intrathymic microenvironments. Immunol Rev 2006;209:10–27. [PubMed: 16448531]

Auerbach R. Analysis of the developmental effects of a lethal mutation in the house mouse. J Exp Zool 1954;127:305–329.

Auerbach R. Morphogenetic interactions in the development of the mouse thymus gland. Dev Biol 1960;2:271–384. [PubMed: 13795076]

Bennett AR, Farley A, Blair NF, Gordon J, Sharp L, Blackburn CC. Identification and characterization of thymic epithelial progenitor cells. Immunity 2002;16:803–814. [PubMed: 12121662]

Blackburn CC, Manley NR. Developing a new paradigm for thymus organogenesis. Nat Rev Immunol 2004;4:278–89. [PubMed: 15057786]

Bleul CC, Boehm T. BMP signaling is required for normal thymus development. J Immunol 2005;175:5213–21. [PubMed: 16210626]

Bockman, DEaKML. Dependence of thymic development on derivative of the neural crest. Science 1984:223.

Conway SJ, Bundy J, Chen J, Dickman E, Rogers R, Will BM. Decreased neural crest stem cell expansion is responsible for the conotruncal heart defects within the splotch (Sp(2H))/Pax3 mouse mutant. Cardiovasc Res 2000;47:314–28. [PubMed: 10946068]

Conway SJ, Henderson DJ, Copp AJ. Pax3 is required for cardiac neural crest migration in the mouse: evidence from the splotch (Sp2H) mutant. Development 1997;124:505–14. [PubMed: 9053326]

Engleka KA, Gitler AD, Zhang M, Zhou DD, High FA, Epstein JA. Insertion of Cre into the Pax3 locus creates a new allele of Splotch and identifies unexpected Pax3 derivatives. Dev Biol 2005;280:396–406. [PubMed: 15882581]

Epstein JA, Li J, Lang D, Chen F, Brown CB, Jin F, Lu MM, Thomas M, Liu E, Wessels A, Lo CW. Migration of cardiac neural crest cells in Splotch embryos. Development 2000;127:1869–78. [PubMed: 10751175]

Erickson M, Morkowski S, Lehar S, Gillard G, Beers C, Dooley J, Rubin JS, Rudensky A, Farr AG. Regulation of thymic epithelium by keratinocyte growth factor. Blood 2002;100:3269–78. [PubMed: 12384427]

Foster K, Sheridan J, Veiga-Fernandes H, Roderick K, Pachnis V, Adams R, Blackburn C, Kioussis D, Coles M. Contribution of neural crest-derived cells in the embryonic and adult thymus. J Immunol 2008;180:3183–9. [PubMed: 18292542]

Franz T. Persistent truncus arteriosus in the Splotch mutant mouse. Anat Embryol (Berl) 1989;180:457–64. [PubMed: 2619088]

Fry TJ, Mackall CL. Interleukin-7: from bench to clinic. Blood 2002;99:3892–904. [PubMed: 12010786]

Gill J, Malin M, Hollander GA, Boyd R. Generation of a complete thymic microenvironment by MTS24 (+) thymic epithelial cells. Nat Immunol 2002;3:635–642. [PubMed: 12068292]

Gordon J, Bennett AR, Blackburn CC, Manley NR. Gcm2 and Foxn1 mark early parathyroid- and thymus-specific domains in the developing third pharyngeal pouch. Mech Dev 2001;103:141–143. [PubMed: 11335122]

Gordon J, Wilson VA, Blair NF, Sheridan J, Farley A, Wilson L, Manley NR, Blackburn CC. Functional evidence for a single endodermal origin for the thymic epithelium. Nat Immunol 2004;5:546–53. [PubMed: 15098031]

Goulding MD, Chalepakis G, Deutsch U, Erselius JR, Gruss P. Pax-3, a novel murine DNA binding protein expressed during early neurogenesis. Embo J 1991;10:1135–47. [PubMed: 2022185]

Graham A, Begbie J, McGonnell I. Significance of the cranial neural crest. Dev Dyn 2004;229:5–13. [PubMed: 14699573]

Hendzel MJ, Wei Y, Mancini MA, Van Hooser A, Ranalli T, Brinkley BR, Bazett-Jones DP, Allis CD. Mitosis-specific phosphorylation of histone H3 initiates primarily within pericentromeric heterochromatin during G2 and spreads in an ordered fashion coincident with mitotic chromosome condensation. Chromosoma 1997;106:348–60. [PubMed: 9362543]

Hollander G, Gill J, Zuklys S, Iwanami N, Liu C, Takahama Y. Cellular and molecular events during early thymus development. Immunol Rev 2006;209:28–46. [PubMed: 16448532]

Itoi M, Tsukamoto N, Yoshida H, Amagai T. Mesenchymal cells are required for functional development of thymic epithelial cells. Int Immunol 2007;19:953–64. [PubMed: 17625108]

Jenkinson WE, Jenkinson EJ, Anderson G. Differential requirement for mesenchyme in the proliferation and maturation of thymic epithelial progenitors. J Exp Med 2003;198:325–32. [PubMed: 12860931]

Jenkinson WE, Rossi SW, Parnell SM, Jenkinson EJ, Anderson G. PDGFRalpha-expressing mesenchyme regulates thymus growth and the availability of intrathymic niches. Blood 2007;109:954–60. [PubMed: 17008543]

Jiang X, Rowitch DH, Soriano P, McMahon AP, Sucov HM. Fate of the mammalian cardiac neural crest. Development 2000;127:1607–16. [PubMed: 10725237]

LeLievre CS, Le Douarin N. Mesenchymal derivatives of the neural crest: analysis of chimaeric quail and chick embryos. J Embryol Exp Morph 1975;34:125–154. [PubMed: 1185098]

Leonard L, Horton C, Maden M, Pizzey JA. Anteriorization of CRABP-I expression by retinoic acid in the developing mouse central nervous system and its relationship to teratogenesis. Dev Biol 1995;168:514–28. [PubMed: 7729586]

Liu C, Saito F, Liu Z, Lei Y, Uehara S, Love P, Lipp M, Kondo S, Manley N, Takahama Y. Coordination between CCR7- and CCR9-mediated chemokine signals in pre-vascular fetal thymus colonization. Blood. 2006

Machado AF, Martin LJ, Collins MD. Pax3 and the splotch mutations: structure, function, and relationship to teratogenesis, including gene-chemical interactions. Curr Pharm Des 2001;7:751–85. [PubMed: 11375778]

Manley NR. Thymus organogenesis and molecular mechanisms of thymic epithelial cell differentiation. Semin Immunol 2000;12:421–428. [PubMed: 11085174]

Moore-Scott BA, Manley NR. Differential expression of Sonic hedgehog along the anterior-posterior axis regulates patterning of pharyngeal pouch endoderm and pharyngeal endoderm-derived organs. Dev Biol 2005;278:323–35. [PubMed: 15680353]

Nagle DL, Martin-DeLeon P, Hough RB, Bucan M. Structural analysis of chromosomal rearrangements associated with the developmental mutations Ph, W19H, and Rw on mouse chromosome 5. Proc Natl Acad Sci U S A 1994;91:7237–41. [PubMed: 8041773]

Ohuchi H, Hori Y, Yamasaki M, Harada H, Sekine K, Kato S, Itoh N. FGF10 acts as a major ligand for FGF receptor 2 IIIb in mouse multi-organ development. Biochem Biophys Res Commun 2000;277:643–9. [PubMed: 11062007]

Pani L, Horal M, Loeken MR. Rescue of neural tube defects in Pax-3-deficient embryos by p53 loss of function: implications for Pax-3- dependent development and tumorigenesis. Genes Dev 2002;16:676–80. [PubMed: 11914272]

Patel SR, Gordon J, Mahbub F, Blackburn CC, Manley NR. Bmp4 and Noggin expression during early thymus and parathyroid organogenesis. Gene Expr Patterns 2006;6:794–9. [PubMed: 16517216]

Revest JM, Suniara RK, Kerr K, Owen JJ, Dickson C. Development of the thymus requires signaling through the fibroblast growth factor receptor R2-IIIb. J Immunol 2001;167:1954–1961. [PubMed: 11489975]

Schaeffer B. Deuterostome Monophyly and Phylogeny. Evolutionary Biology 1987;21:179–235.

Shinohara T, Honjo T. Studies in vitro on the mechanism of the epithelial/mesenchymal interaction in the early fetal thymus. Eur J Immunol 1997;27:522–529. [PubMed: 9045926]

Tsai PT, Lee RA, Wu H. BMP4 acts upstream of FGF in modulating thymic stroma and regulating thymopoiesis. Blood 2003;102:3947–53. [PubMed: 12920023]

Veitch E, Begbie J, Schilling TF, Smith MM, Graham A. Pharyngeal arch patterning in the absence of neural crest. Curr Biol 1999;9:1481–4. [PubMed: 10607595]

Zamisch M, Moore-Scott B, Su DM, Lucas PJ, Manley N, Richie ER. Ontogeny and regulation of IL-7-expressing thymic epithelial cells. J Immunol 2005;174:60–7. [PubMed: 15611228]

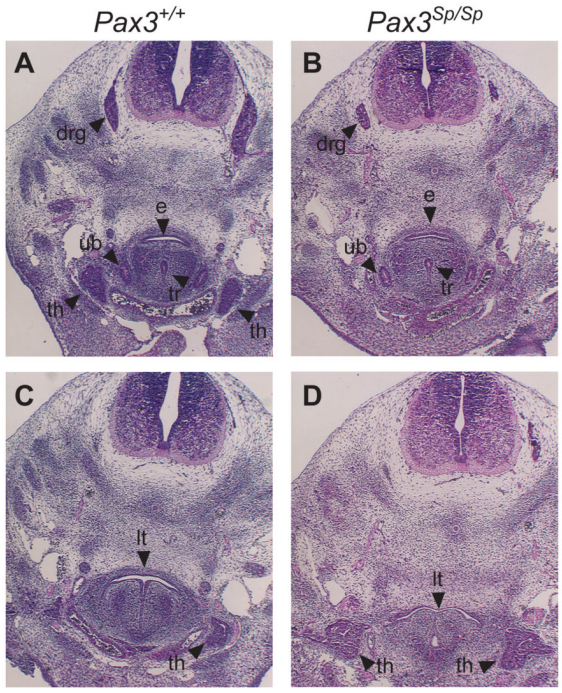

G	Thymus Volume ($10^{-4}mm^3$)	No. Lobes	P Value
Pax3$^{+/+}$	121.4±39.7	4	
Pax3$^{Sp/Sp}$	174.2±29.9	4	<0.01

H	Parathyroid Volume ($10^{-4}mm^3$)	No. Lobes	P Value
Pax3$^{+/+}$	1.88±0.05	4	
Pax3$^{Sp/Sp}$	1.09±0.81	4	<0.05

Figure 1. Thymus lobes in *Pax3*$^{Sp/Sp}$ embryos are large and ectopic

(**A–D**) Transverse H&E stained sections from E12.5 embryos. Dorsal is up. *Pax3*$^{+/+}$ thymus lobes are located cranial to the heart and posterior to the laryngeo-tracheal groove (**A**). Thymus lobes are not evident at a comparable position in the *Pax3*$^{Sp/Sp}$ embryo (**B**). Hypoplastic dorsal root ganglia are apparent in *Pax3*$^{Sp/Sp}$ embryos. Cranial sections, reveal large, ectopic thymus lobes in *Pax3*$^{Sp/Sp}$ mutant (**D**), whereas only the anterior tip of one lobe is evident in the wildtype littermate (**C**). 3-D reconstructions of *Pax3*$^{+/+}$ (**E**) and *Pax3*$^{Sp/Sp}$ (**F**) pharyngeal regions showing thymus (red), parathyroid (green), esophagus (blue) and trachea (yellow). Average volume of *Pax3*$^{+/+}$ and *Pax3*$^{Sp/Sp}$ thymic (**G**) and parathyroid lobes (**H**).

Abbreviations are drg, dorsal root ganglia; e, esophagus; tr, trachea ; th, thymus; lt, laryngeo-tracheal groove; ub, ultimobranchial bodies.

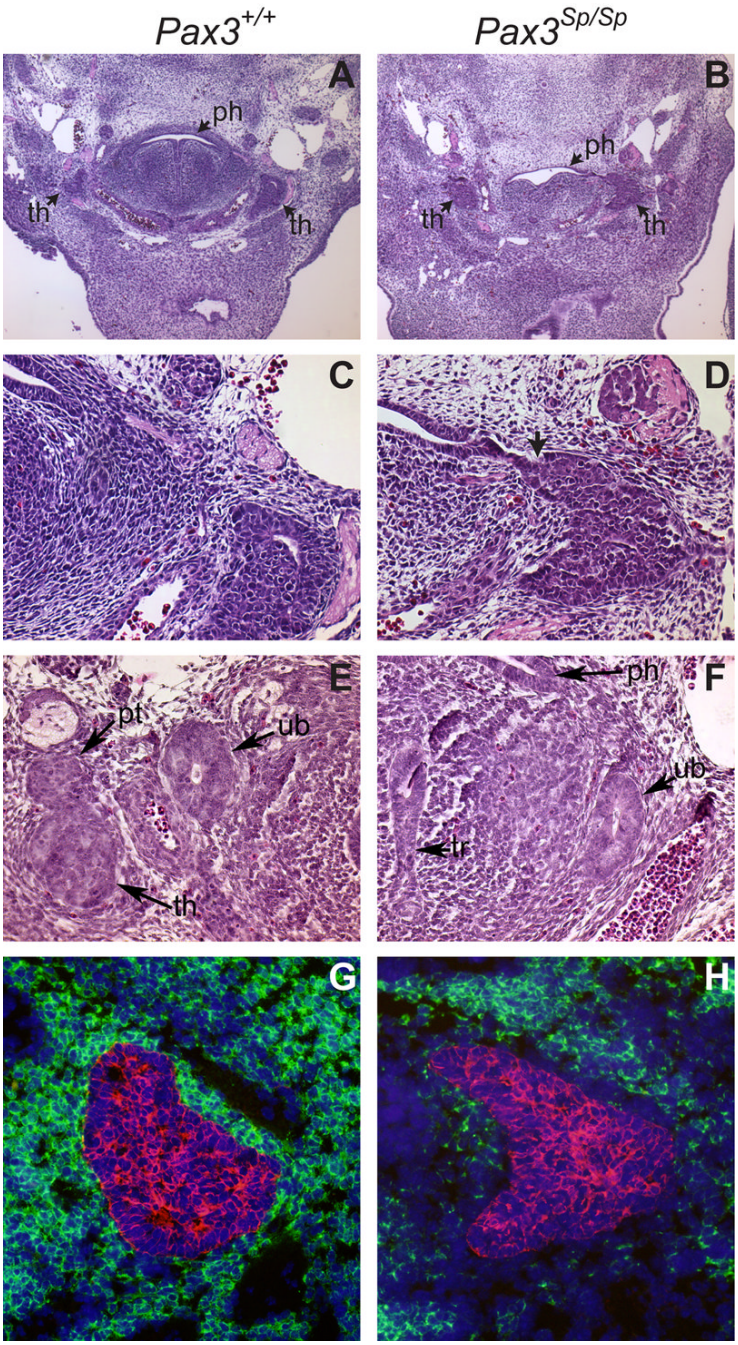

Figure 2. Delayed detachment phenotype is specific to the third pouch

Transverse H&E stained sections from (**A,C,E**) *Pax3*$^{+/+}$ and (**B,D,F**) *Pax3*$^{Sp/Sp}$ E12.5 embryos. Panels C and D are higher magnification (20X) images of A and B (5X). The arrow in D shows attachment of *Pax3*$^{Sp/Sp}$ thymus rudiment to the pharynx. Normal ultimobranchial body detachment occurs in *Pax3*$^{+/+}$ and *Pax3*$^{Sp/Sp}$ embryos (**E,F**). Abbreviations are thymus (th), parathyroid (pt), pharynx (ph) and ultimobranchial body (ub). Transverse frozen sections from (**G**) *Pax3*$^{+/+}$ and (**H**) *Pax3*$^{Sp/Sp}$ E12.5 embryos were stained with anti-PDGFRα (green), anti-pancytokeratin (red) and DAPI (blue).

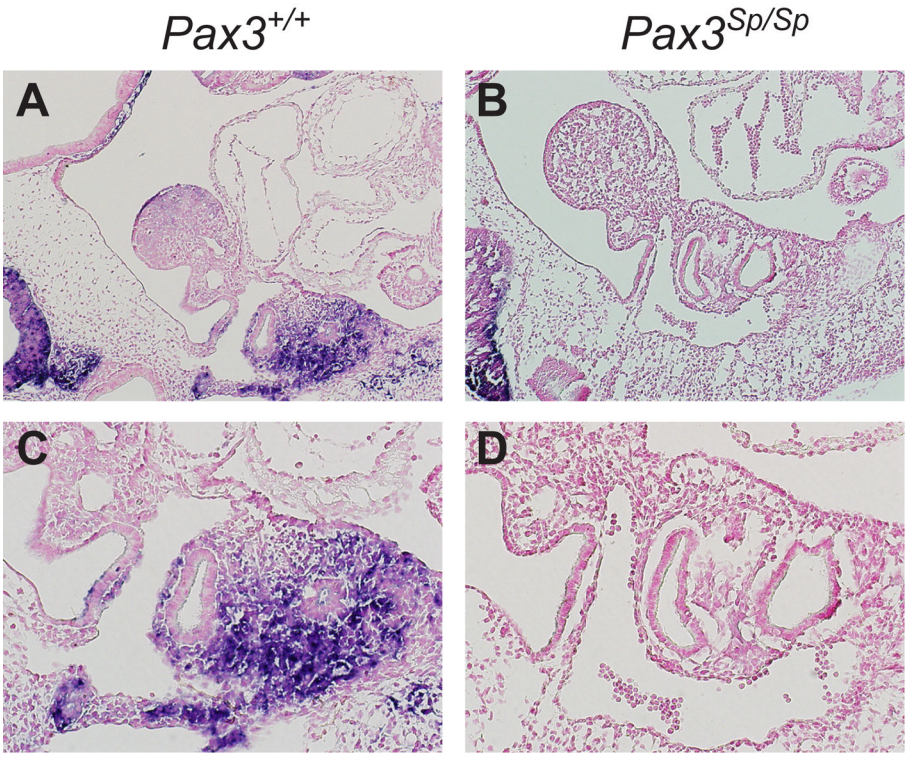

Figure 3. NCC localization is disrupted at E10.5 in Pax3$^{Sp/Sp}$ embryos

Sagittal sections from E10.5 *Pax3*$^{+/+}$(**A,C**) and *Pax3*$^{Sp/Sp}$ (**B,D**) embryos were incubated with anti-sense riboprobe for *CrabP1* to detect migrating NCC. (**C and D**) are higher magnification views of the third pouch region. Cranial is up and ventral is left. The clear space surrounding the pouches is an artifact of tissue processing. There is a paucity of *CrabP1* expressing NCCs in pharyngeal arches and pouches of *Pax3*$^{Sp/Sp}$ embryos.

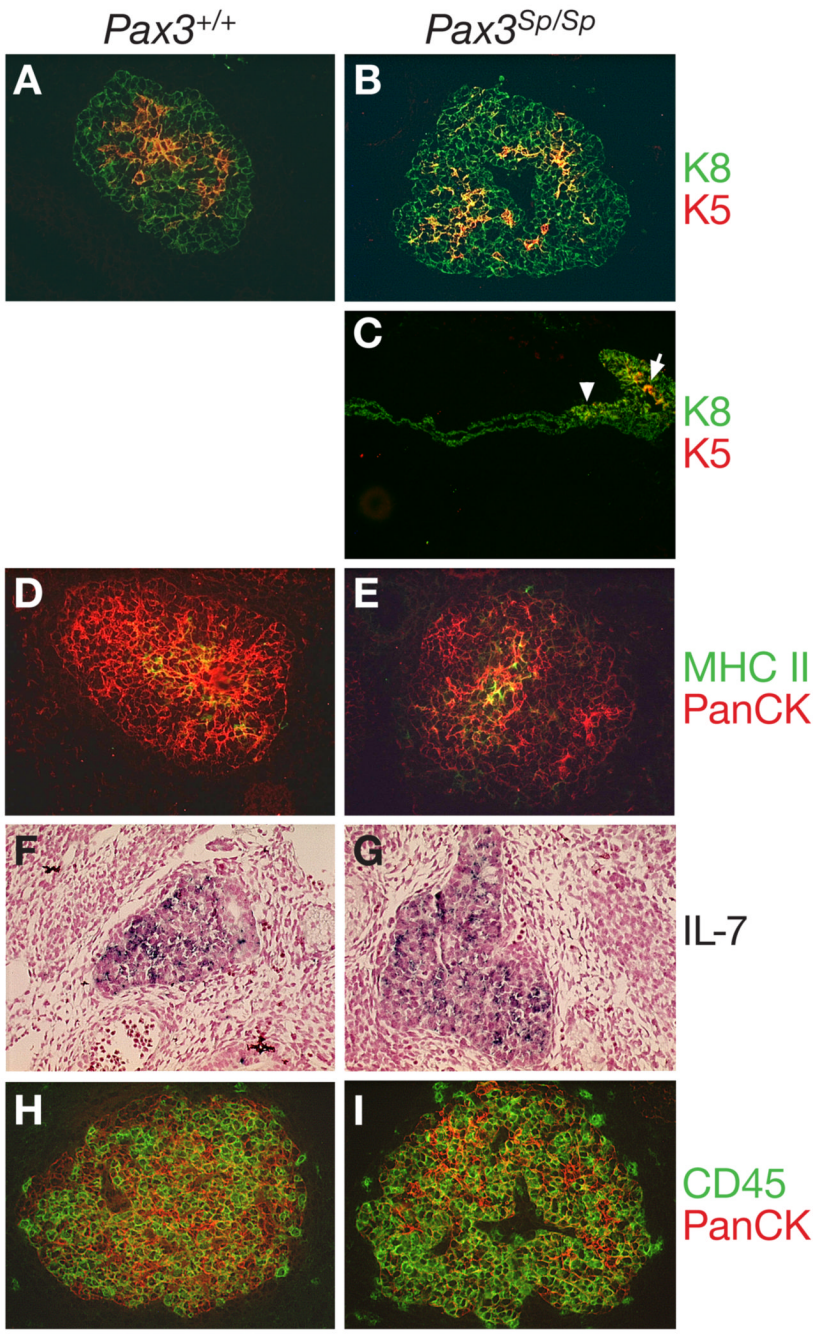

Figure 4. Epithelial differentiation is normal in E12.5 in *Pax3*$^{Sp/Sp}$ thymus lobes

Transverse frozen sections from wild type (**A**) and *Pax3*$^{Sp/Sp}$ embryos (**B,C**) stained with anti-K5 (red) or anti-K8 (green). Note the presence of $K8^{+}K5^{+}$ epithelial cells in the center of the *Pax3*$^{Sp/Sp}$ rudiment (arrow) even when it remains attached to the pharyngeal endoderm (arrowhead). Frozen thymus sections form *Pax3*$^{+/+}$ (**D**) and *Pax3*$^{Sp/Sp}$ (**E**) embryos stained with anti-MHC class II (green) and anti-pan-cytokeratin (red). ISH analysis of *IL-7* expression in sagittal sections of E12.5 thymus from *Pax3*$^{+/+}$ (**F**) and *Pax3*$^{Sp/Sp}$ (**G**) embryos. Frozen transverse sections from *Pax3*$^{+/+}$ (**H**) and *Pax3*$^{Sp/Sp}$ (**I**) E12.5 embryos stained with anti-CD45 (green) and anti-pan-cytokeratin (red).

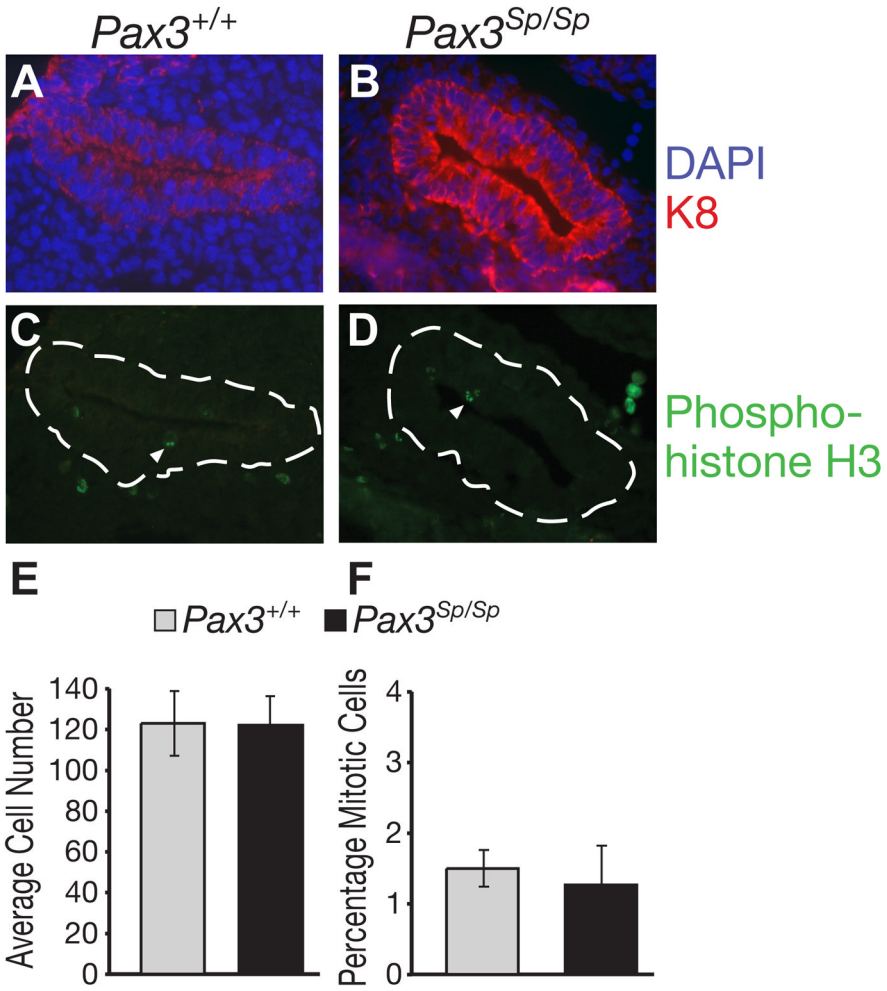

Figure 5. Proliferation and cellularity in *Pax3*$^{Sp/Sp}$ common primordia

Sagittal sections of E11.5 *Pax3*$^{+/+}$(**A, C**) and *Pax3*$^{Sp/Sp}$ (**B, D**) embryos; cranial is up and dorsal is right. Staining for K8 (red) reveals epithelial cells in the common primordium; DAPI staining (blue) detects nuclei (**A,B**). Mitotic cells detected by costaining with anti-phosphohistone H3 antibody (green) (**C,D**). Average cell number (**E**) and percentage of mitotic cells (**F**) per section were determined by counting multiple sections from three *Pax3*$^{+/+}$ and three *Pax3*$^{Sp/Sp}$ embryos.

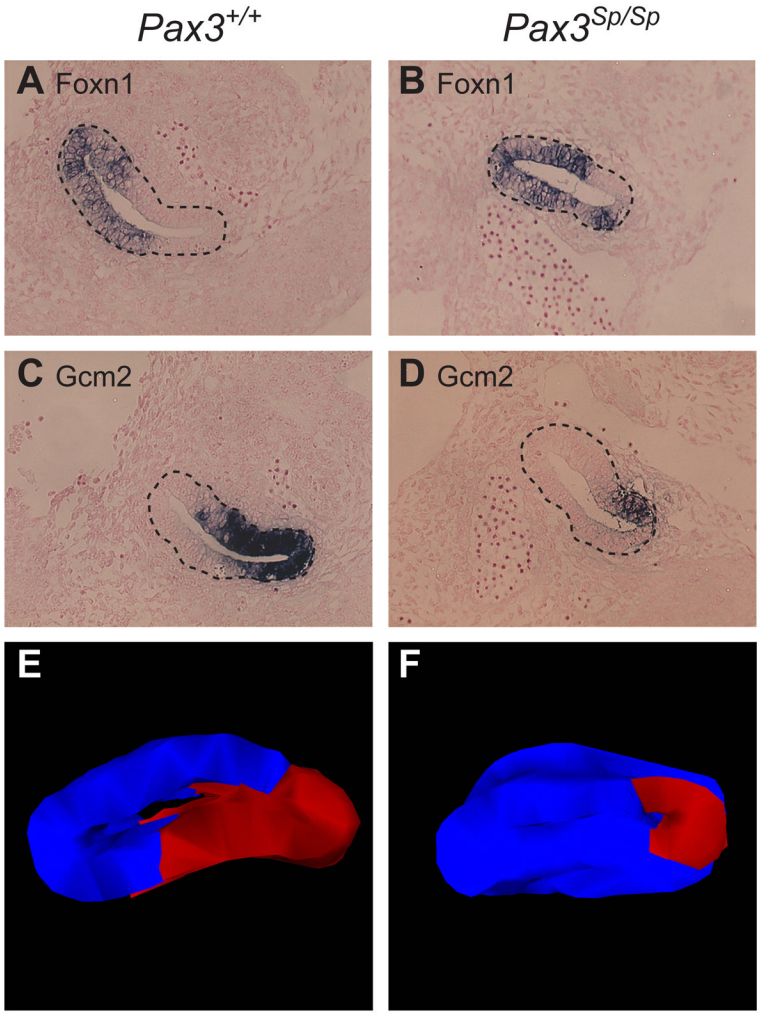

G	3rd PP Volume ($10^{-4}mm^3$)	No. Pouches	P Value
***Pax3*$^{+/+}$**	59.7±1.0	4	
***Pax3*$^{Sp/Sp}$**	61.9±0.9	4	>0.75

Figure 6. Thymus/parathyroid fate boundary is shifted in *Pax3*$^{Sp/Sp}$ third pharyngeal pouch

Sagittal sections of E11.5 *Pax3*$^{+/+}$(**A,C**) and *Pax3*$^{Sp/Sp}$ (**B,D**) embryos analyzed by ISH for *FoxN1* (**A,B**) and *Gcm2* (**C,D**). The third pouch is indicated by a dotted line. Cranial is up and ventral is to the left. 3-D reconstructions of *FoxN1* (blue) and *Gcm2* (red) expression domains (**E,F**). Average volume of *Pax3*$^{+/+}$ and *Pax3*$^{Sp/Sp}$ third pharyngeal pouch (**G**).

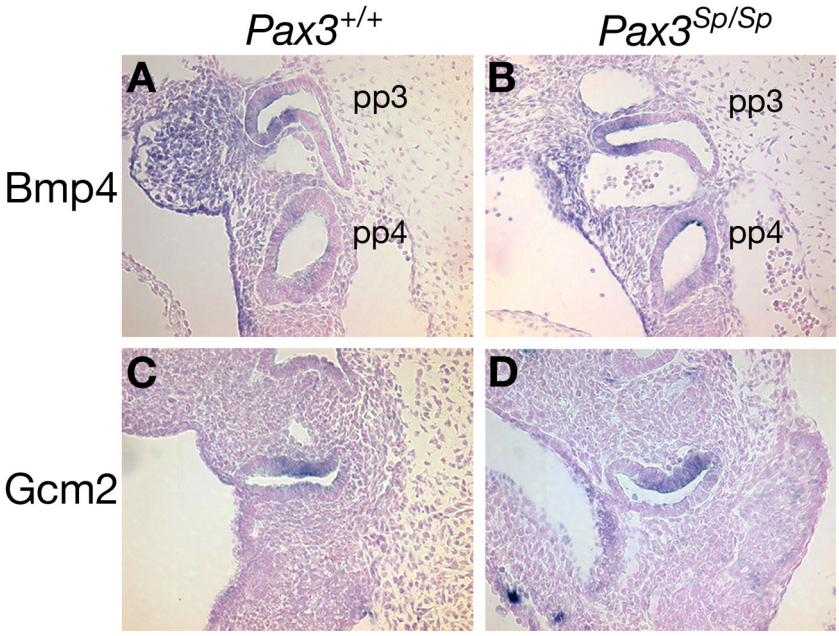

Figure 7. Third pharyngeal pouch patterning is normal at E10.5 in Pax3$^{Sp/Sp}$ embryos

Sagittal sections from *Pax3*$^{+/+}$ (A,C) and *Pax3*$^{Sp/Sp}$ (B,D) embryos at E10.5 were stained by ISH with anti-sense riboprobe for *Bmp4* (A,B) or *Gcm2* (C,D) and counterstained with nuclear fast red. In all panels, ventral is left and cranial is up. pp3, third pharyngeal pouch; pp4, fourth pharyngeal pouch. Neither *Bmp4* nor *Gcm2* expression is changed in the mutants.

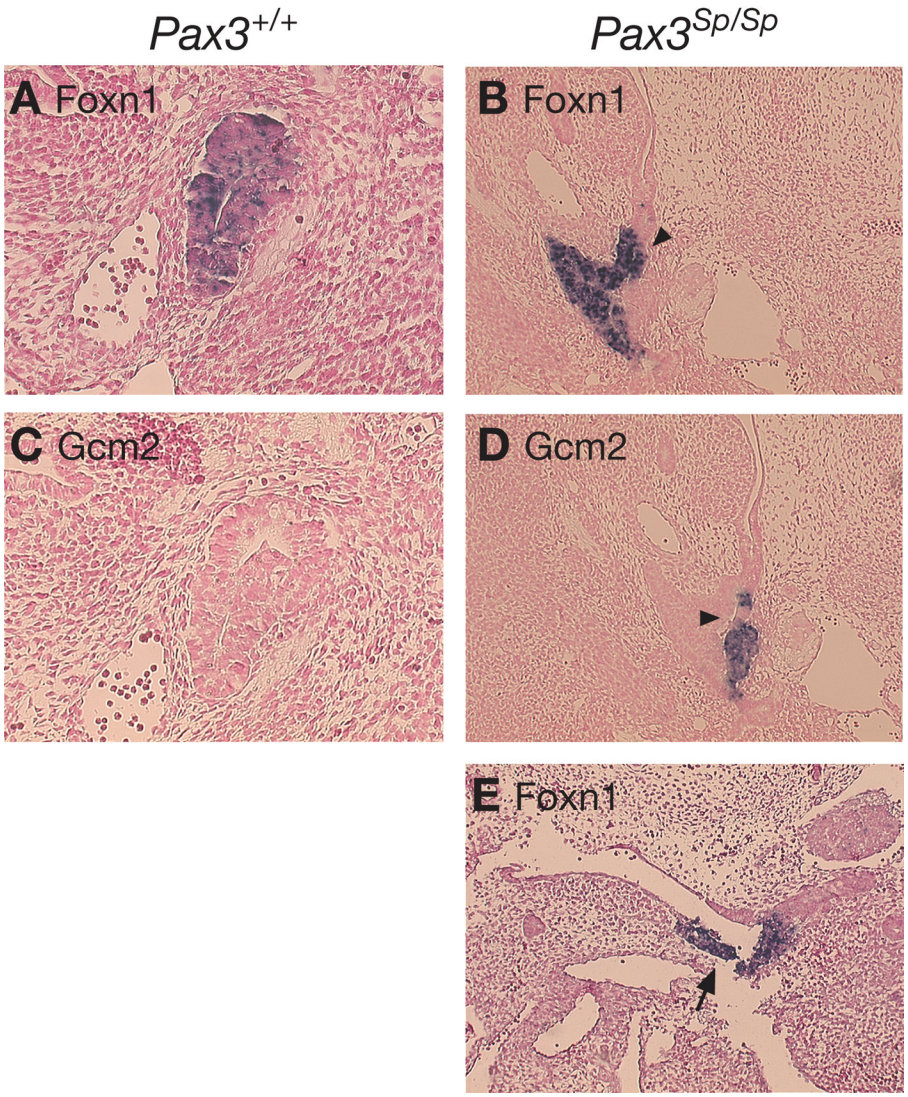

Figure 8. Delayed separation and mixing of thymus and parathyroid fate domains in E12 *Pax3*$^{Sp/Sp}$ embryos

Transverse sections of E12.0 *Pax3*$^{+/+}$ (**A,C**) and *Pax3*$^{Sp/Sp}$ (**B,D,E**) littermates analyzed for *FoxN1* (**A,B,E**) and *Gcm2* (**C,D**) expression by ISH. Ventral is down in (**A–E**). Arrowheads in **B** and **D** indicate mixing of *FoxN1* and *Gcm2* domains in *Pax3*$^{Sp/Sp}$ embryos. Note that the common primordium remains attached to the pharynx. (**E**) *FoxN1* expression in *Pax3*$^{Sp/Sp}$ embryo extends into the pharyngeal endoderm exterior to the pouch.

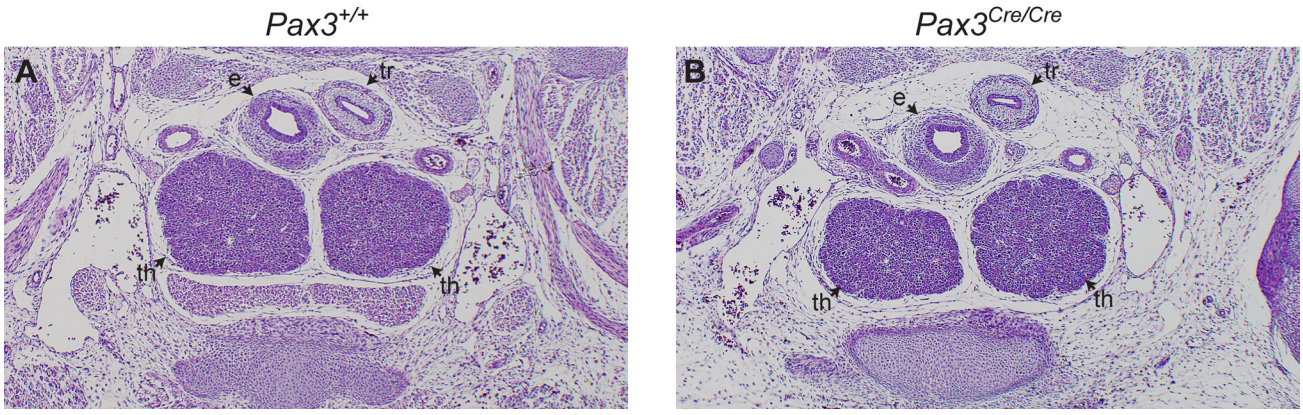

Figure 9. Thymus lobes in E14.5 *Pax3*$^{Cre/Cre}$ embryos

Transverse H&E stained sections from E14.5 *Pax3*$^{+/+}$ (**A**) and *Pax3*$^{Cre/Cre}$ (**B**) embryos. Abbreviations are; e, esophagus; tr, trachea ; th, thymus.